Food and Chemical Toxicology 121 (2018) 237–245

Contents lists available at ScienceDirect

Food and Chemical Toxicology

journal homepage: www.elsevier.com/locate/foodchemtox

Lyophilized açaí pulp (*Euterpe oleracea* Mart) attenuates colitis-associated colon carcinogenesis while its main anthocyanin has the potential to affect the motility of colon cancer cells

Mariana F. Fragoso[a,*], Guilherme R. Romualdo[a], Lisa A. Vanderveer[b], Janusz Franco-Barraza[c], Edna Cukierman[c], Margie L. Clapper[b], Robson F. Carvalho[d], Luis F. Barbisan[d]

[a] Department of Pathology, Botucatu Medical School, UNESP, Botucatu, SP, Brazil
[b] Cancer Prevention and Control Program, Fox Chase Cancer Center, Philadelphia, PA, USA
[c] Cancer Biology Program, Fox Chase Cancer Center, Philadelphia, PA, USA
[d] Department of Morphology, Institute of Biosciences of Botucatu, UNESP, Botucatu, SP, Brazil

ARTICLE INFO

Keywords:
Lyophilized açaí pulp
Cyanidin 3-rutinoside
Colon carcinogenesis
Colitis
Prevention

ABSTRACT

This study evaluated the possible protective effects of lyophilized açaí pulp (AP) in a colitis-associated carcinogenesis (CAC) rat model and the modifying effect of cyanidin 3-rutinoside (C3R) on the motility of RKO colon adenocarcinoma cells, using the wound healing assay. Male Wistar rats were induced to develop CAC using 1,2-dimethylhydrazine (DMH) and 2,4,6-trinitrobenzene acid (TNBS). Animals were randomly assigned to different groups that received basal diet or basal diet supplemented with 5.0% or 7.5% lyophilized AP. The findings indicate: 1) C3R (25 μM) has the potential to reduce RKO cell motility *in vitro*; 2) ingestion of lyophilized AP reduces the total number of aberrant crypt foci (ACF), ACF multiplicity, tumor cell proliferation and incidence of tumors with high grade dysplasia; 3) AP increases the gene expression of negative regulators of cell proliferation such as Dlc1 and Akt3, as well as inflammation (Ppara). Thus, lyophilized AP could exert a potential antitumor activity.

1. Introduction

Colorectal cancer (CRC) is one of the most common neoplasias in the industrialized world (Torre et al., 2015). It is estimated that 16,660 men and 17,620 women were diagnosed with CRC in Brazil in 2016 (INCA, 2016). Epidemiological and experimental evidence indicate that a sedentary life style and poor dietary habits, including a high intake of red and processed meat and a low intake of fiber, increase one's risk for CRC (Lofano et al., 2012). Genetic and epigenetic alterations in colonic epithelial cells lead to the onset of sporadic, hereditary or inflammatory bowel disease (IBD) (Das et al., 2007).

Prolonged exposure to inflammatory processes in the context of IBD can increase the risk of developing CRC (Femia and Caderni, 2008). Several animal models, including transgenic, immunodeficient and chemically-induced models, have been established to enhance our understanding of the events that promote inflammation-associated carcinogenesis (Femia and Caderni, 2008). In general, chemically-induced models of CRC employ an inducer of inflammation in combination with a carcinogen. For example, one of these models utilizes trinitrobenzene sulfonic acid (TNBS) to induce inflammation and 1,2-dimethylhydrazine (DMH), a colon carcinogen (Santiago et al., 2007).

Due to the high incidence of CRC globally and associated mortality, significant effort has focused on developing preventive strategies to attenuate or inhibit CRC, especially via consumption of natural compounds (Paz et al., 2015). Animal models of CRC represent an ideal system in which to evaluate the effects of pharmacological or natural products on the development and/or progression of CRC (Femia and Caderni, 2008).

Açaí (*Euterpe oleraceae* Mart) is a dark purple, berry-like fruit that grows on large palm trees that are indigenous to South America and can be found in the Brazilian Amazon floodplains (Schauss et al., 2006). In the Northern region of Brazil, consumption can be as high as 2 L/day (Kahyat, 2005). Results from a recent study indicate that açaí is one of the major antioxidants in the Brazilian diet (Torres and Farah, 2016).

* Corresponding author.
E-mail addresses: mariana.fragoso@fccc.edu (M.F. Fragoso), romualdo.gr15@gmail.com (G.R. Romualdo), Lisa.Vanderveer@fccc.edu (L.A. Vanderveer), Janusz.FrancoBarraza@fccc.edu (J. Franco-Barraza), Edna.Cukierman@fccc.edu (E. Cukierman), Margie.Clapper@fccc.edu (M.L. Clapper), rcarvalho@ibb.unesp.br (R.F. Carvalho), barbisan@ibb.unesp.br (L.F. Barbisan).

https://doi.org/10.1016/j.fct.2018.08.078
Received 31 January 2018; Received in revised form 24 August 2018; Accepted 31 August 2018
Available online 06 September 2018
0278-6915/

This “super fruit” has received significant public attention because of its potential antioxidant and anti-inflammatory properties (Schauss et al., 2006).

Studies characterizing the phytochemical composition of this berry-like fruit (Romualdo et al., 2015; Schauss et al., 2006) have attributed its biological properties to anthocyanins, especially cyanidin 3-glucoside (C3G), cyaniding 3-rutinoside (C3R) and carotenoids (Romualdo et al., 2015). Anthocyanins, glycosides of anthocyanidins, are responsible for the dark purple color of the açaí fruit, as well as its antioxidant activity (Yamaguchi et al., 2015). The main anthocyanins of the açaí fruit have been evaluated for their potential anti-tumor activity in different *in vivo* and *in vitro* bioassays (Fragoso et al., 2013; Romualdo et al., 2015; Yamaguchi et al., 2015). Besides anthocyanins, the açaí fruit also possesses large amounts of liposoluble carotenoids (Romualdo et al., 2015), one of the major classes of plant pigments with antioxidant activity (Milani et al., 2017).

Although consumption of açaí fruit pulp has increased in Brazil and worldwide, few mechanistic studies have assessed its anti-tumor activity in rodent models of chemically-induced carcinogenesis (Ribeiro et al., 2010; Fragoso et al., 2013; Romualdo et al., 2015). The present study was performed to: 1) determine if lyophilized açaí pulp (AP), a putative inhibitor of oxidative stress, is efficacious in reversing chemically-induced CRC carcinogenesis associated with acute inflammation *in vivo*; and 2) evaluate the ability of cyanidin 3-rutinoside to alter the motility of human RKO colon carcinoma cells *in vitro*.

2. Materials and methods

2.1. Chemicals and compounds

1,2-Dimethylhydrazine hydrochloride (DMH), N-acetyl-L-cysteine (NAC) and 2,4,6-trinitrobenzenesulfonic acid solution (TNBS) were obtained from Sigma-Aldrich (St. Louis, MO, USA). Cyanidin 3-rutinoside chloride (C3R) (purity: ≥98%; Molecular weight: 630.98; Molecular formula: $C_{27}H_{31}C\ell O_{15}$) was obtained from Santa Cruz Biotechnology (CAS, 18719-76-1), diluted in 1.6 mL of nuclease-free water (final concentration 1 μM), and stored at −20 °C. Açaí pulp was harvested from Belém - PA (Brazil) and samples were lyophilized by Liotécnica Food Technology (Embu das Artes - SP, Brazil).

2.2. Experimental diets

Four different experimental diets were used: (1) A cereal-based commercial rodent diet (Nuvilab-CR1, Nuvital-PR) alone or complemented with: (2) 0.2% (0.2 g/kg chow) N-acetylcysteine (Sigma-Aldrich, USA), (3) 5.0% (50 g/kg chow) or (4) 7.5% (75 g/kg chow) lyophilized AP (Liotécnica - Food Technology). After complete homogenization using an industrial mixer (CAF model M60), experimental diets were pelleted (Chavantes– PR, Brazil) using dry ventilation, packed in pre-labeled plastic bags, and stored under refrigeration. Food cups were replenished with fresh diet twice a week. All animals received filtered water and food *ad libitum*.

2.3. Experimental design

All experiments were conducted in accordance with the Ethical Principles for Animal Research adopted by the Brazilian College of Animal Experimentation (COBEA). The experimental protocols were approved by the Ethics Committee for Animal Research (protocol number CEEA 1041-2013) at Botucatu Medical School (FMB/UNESP). As shown in Fig. 1, male Wistar rats were randomly assigned to four groups and received: (G1) basal diet (n = 20); (G2) basal diet supplemented with 0.2% NAC (N-acetylcysteine, a known chemopreventive agent and positive control [Amrouche-Mekkioui and Djerdjouri, 2012]) (n = 15); (G3 and G4), basal diet supplemented with 5.0% or 7.5% lyophilized AP, respectively (n = 20 each group). At weeks 1 and 2, rats received 4 doses of DMH (40 mg/kg), twice a week. Two weeks after receiving DMH, acute inflammation was induced by administrating intra-rectally 10 mg of TNBS dissolved in 0.25 mL of 50% ethanol (v/v) in the middle colon to accelerate the carcinogenesis process. Dietary interventions were introduced at week 3. Forty-eight hours after induction of colitis, rats (5/group) were euthanized for confirmation of the inflammatory process via gross observation and histological assessment. The remaining animals were euthanized by week 25 and macroscopically-identified colon tumors were measured and processed for histopathological assessment, immunohistochemical staining and gene expression analyses (Fig. 1).

2.4. Quantification and characterization of anthocyanins and carotenoids

The amount of anthocyanin in the experimental AP was determined according to the Hendry and Houghton protocol (1992). Anthocyanins were extracted by incubating 10 mg of sample with 10 mL of methanol acidified with formic acid (1:9 v/v) in an ultrasonic bath, followed by centrifugation to achieve solution discoloration. Aliquots of 400 μL were lyophilized. Absorbance was measured at 450 and 600 nm using a UV/vis GBC911A spectrophotometer; an ethanol-HCℓ 1.5 N solution (85:15) served as a reference [extinction factor 98.2 cm^{-1} $(mg/ml)^{-1}$].

Samples of 100 μL of anthocyanin extract were diluted in 5% formic acid in water:methanol (90:10). The analyses were performed in triplicate using a Waters Alliance 2695™ system, including a Waters™ 2996 diode array detector and column (Thermo Scientific™ BDSC18; 100 mm × 4.6 mm, 2.4 mm), at a flow rate of 1.0 mL min^{-1}, column temperature of 40 °C, injection volume of 20 μL and gradient elution method with acetonitrile and formic acid. The majority of anthocyanins were quantified via external standardization.

Carotenoids were quantified and characterized according to the Rodriguez-Amaya method (2001). Four grams of AP matrix was macerated in porcelain grails with 3 g of celite and 50 mL of acetone. The sample was vacuum-filtered onto a sintered glass funnel plate. The acetone extract was transferred to a beaker containing 50 mL of petroleum ether and washed with 300 mL of ultrapure water. The extract was filtered with anhydrous sodium sulfate and 100 mL was collected in a flask filled with petroleum ether. The total carotenoid level of the sample was determined via spectrophotometry at 450 nm (Shimadzu UV-1900, Shimadzu, Japan).

The profile of carotenoids was determined in a 1 mL aliquot. The sample was dried under a stream of nitrogen and dissolved in 100 mL of acetone. The solution was homogenized for 10 s and then subjected to HPLC analysis using a Water/HPLC system controlled by Empower software and a Waters™ diodes 996 array detector. Carotenoids were isolated using a C30 column (S-3 carotenoid, 4.6 mm × 250 mm, YCM), with a gradient elution of methanol and methyl tert-butyl ether. The flow rate was 0.8 mL min^{-1} and the race was 28 min. The sample injection volume was 15 μL. Carotenoids were identified based on their retention time and UV absorption spectrum/Vis when compared with the retention time of commercial standards of carotenoids.

2.5. Histological processing and immunohistochemistry protocol

At the end of the experiment, the animals were euthanized, and the colons were excised and washed with saline to remove fecal residue. The colons were examined grossly and tumors were counted and measured. Colon tumors were banked stored for molecular analysis and the remainder of the colon was fixed in 10% buffered formalin for 24 h at room temperature. After fixation, the colons were swiss-rolled, embedded in paraffin, and sectioned for histological evaluation by hematoxylin-eosin (HE) staining and immunohistochemical staining for Ki-67, β-catenin and Connexin 43 (Cx43), as described (Fragoso et al., 2013). The liver was also removed and weighed, and peripheral blood samples were collected in order to measure serum alanine amino transferase (ALT) using an automated kinetic method (Cobas C501—

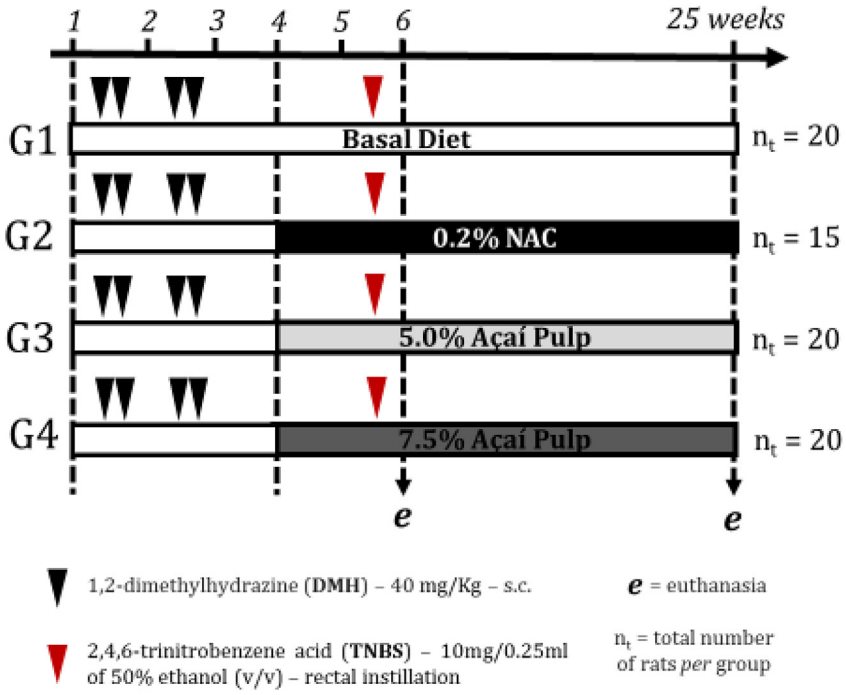

Fig. 1. Experimental design. G1: DMH + TNBS [2,4,6-trinitrobenzene acid] + basal diet (n = 20); G2: DMH + TNBS + basal diet with 0.2% NAC [N-acetylcysteine] (n = 15); G3: DMH + TNBS + basal diet with 5% lyophilized açaí pulp (AP) (n = 20); G4: DMH + TNBS + basal diet with 7.5% AP (n = 20).

Roche, USA) (n = 5/group).

2.6. Aberrant crypt foci (ACF) analyses

Stereoscopic analysis of classical ACF was performed in colon whole mounts stained with 1.0% methylene blue dissolved in phosphate-buffered saline (PBS) (Fragoso et al., 2013). ACF were identified according to Bird's criteria (Bird and Good, 2000). The number of ACF with 1–3, 4-10 and > 10 aberrant crypts (ACs), as well as the total number of ACs and ACF were determined.

2.7. Apoptosis, Ki-67, β-catenin and connexin 43 analyses

The apoptotic index (AI) of H&E-stained colon tumor sections (5 tumors/group) was calculated as the number of apoptotic cells divided by the total number of cells counted X 100. The cell proliferation index (Ki-67 labeling index (Ki-67 LI) was defined as the number of stained cells divided by the total cells counted X 100. Tumor cells were scored as positive or negative for membranous, cytoplasmic or nuclear immunostaining of β-catenin and Connexin 43, and compared with adjacent unaltered colonic crypts (Fragoso et al., 2013).

2.8. Histopathology analysis

H&E stained sections of macroscopic colon tumors and Swiss-rolled colon segments (2–3.2-mm in width) were examined histologically to determine the morphological type of tumor. Tumors were evaluated in a blinded manner based on the phenotype, grading, pattern of growth and presence of dysplasia (high and low), as described previously (Hamilton and Aaltonen, 2000).

2.9. RNA extraction from tumors

Approximately 30 mg of each tumor was homogenized in 1 mL QIAzol (QIAGEN, Crawley, UK) using a homogenizer (Biospec Products, INC., Bartlesville, OK 74005). RNA fractions were isolated separately using a commercial column-based system according to the manufacturer's instructions (QIAGEN RNeasy® Mini Kit, QIAGEN Inc. USA Valencia, CA - USA). RNA quantification and quality control analyses were assessed using NanoVue spectrophotometry (GE Healthcare UK Limited, UK) ($Abs_{260/280}$ value of 1.95 ± 0.19) and the Agilent 2100 Bioanalyzer (RIN value of 8.89 ± 1.0), respectively. The remaining RNA was stored at −80 °C until further use.

2.10. cDNA synthesis and TaqMan® Array Cards (TAC)-based real-time polymerase chain reaction (qRT-PCR)

cDNA was synthesized from ≤2 μg of total RNA using MultiScribe™ Reverse Transcriptase (Applied Biosystems, USA). RNA expression profiles were analyzed using 96-well TaqMan® Array Cards (TAC)-based real-time polymerase chain reaction (PCR). The custom TAC consisted of 96 genes (91 targets genes and 5 reference genes) involved in regulation of cell proliferation and differentiation, self-sufficiency in growth signals, insensitivity to inhibitory growth signals, avoidance of apoptosis, unlimited replicative potential, sustained angiogenesis and invasiveness (metastasis). Five samples from each treatment group were analyzed. Target genes were amplified using the TaqMan® Universal Mastermix II (Life Technologies, USA). The cycling protocol included heat activation at 50 °C for 1 min and denaturation at 95 °C for 10 min, followed by 40 cycles of 95 °C for 15 s and 60 °C for 1 min. Fluorescence detection was performed on a QuantStudio™ 12 K Flex Real-Time PCR System (Life Technologies, USA). Relative quantitation was calculated based on the $2^{-(\Delta\Delta Ct)}$ method (Livak and Schmittgen, 2001), using Expression Suite Software v1.1 (Life Technologies, USA). Normalization was performed using the most stable reference genes (*18S*, *Actb* and *Gusb*) based on geNorm calculation (Vandesompele et al., 2002).

2.11. Cell culture and cell viability

RKO human colon adenocarcinoma cells were obtained from the American Type Culture Collection (ATCC) and grown in Eagle's Minimum Essential Medium (2,2 g/L $NaHCO_2$, pH 7.2) (Fox Chase Cancer Center Cell Culture Facility, USA), complemented with 10% Fetal Bovine Serum (FBS), 100 U/mL penicillin and 100 μg/mlL

streptomycin. Cells were cultured in T-75 plastic flasks (Corning Life Sciences, Asia Pacific) at 37 °C in 5% CO_2. Once they reached ~85% confluency, cells were harvested by trypsinization (0.25% trypsin, in Ca^{++} and Mg^{++} free PBS, pH 7.4) and seeded at 3×10^5 cells/well in 6-well plates, until 95% confluency was obtained.

To analyze cell viability, tumor cells were cultured in triplicate for 24 h (2×10^3 cells/well) in a 96-well plate and incubated with AlamarBlue®, according to the manufacturer's instructions (AlamarBlue® Cell Viability Reagent, Invitrogen, UK). Plates were scanned using a microplate reader (Tecan) and Magellan software version 6.6. Cell viability was determined by plotting normalized absorbance at 570 nm versus compound concentration. A direct correlation exists between absorbance values and total metabolic activity.

2.12. Wound healing assay

Confluent monolayers of tumor cells were scratched with a plastic tip across each well. Debris and floating cells were removed, and serum-free media was used to reduce cell proliferation during the analysis. This was used to normalize the wound healing assay assuming that closure was due to migration and not proliferation. Cells were treated with 25, 50 or 100 μM C3R. Wound closure was evaluated at 24 and 48 h using a phase contrast Nikon Eclipse TE2000-U inverted microscope, with a 20× objective, equipped with a Photometrics cool snap HQ CCD camera. Images were acquired using MetaMorph version 6.2r6 software. A total of eight pictures per condition were obtained from random areas of the well and assessed using ImageJ version 1.50b (https://imagej.nih.gov/ij/).

2.13. Statistical analysis

All data were analyzed by One-Way ANOVA and *post hoc* Tukey or Dunn's test, except for tumor incidence, which was analyzed by Chi-square or Fisher's Exact Test. $P < 0.05$ was selected as the criterion of significance.

3. Results

3.1. Lyophilized AP is rich in anthocyanins and carotenoids

Characterization of AP indicated that the most abundant anthocyanin was cyanidin 3-rutinoside (C3R) (214.09 ± 17:32 mg/100 g) (Fig. 2A and Table 1). In addition to anthocyanins, the carotenoids in lyophilized AP were also characterized (Table 1 and Fig. 2B). As listed in Table 1, the most abundant carotenoid was β-carotene (1908.5 ± 24.4 mg/100 g). C3R was chosen to be tested in the wound healing assay, as the focus of this study was on the effects of anthocyanins.

3.2. C3R interfered with RKO tumor cell motility in vitro

To assess the *in vitro* effects of C3R on cell motility, we selected a colon carcinoma cell line (RKO) that is poorly differentiated and exhibits high invasive potential (Feng et al., 2012). RKO cells were treated with C3R and each treatment group was evaluated at two time-points (intragroup analysis): 0 h–24 h, and 24 h–48 h (Fig. 3SA). Cell motility was detected under all conditions ($p < 0.001$) and at both time-points, except for the group treated with 25 μM C3R that presented a modest reduction in cell motility between 24 h and 48 h of experiment ($p = 0.0579$, not statistically significant, meaning there was no cell movement during this period). This result suggests that the effect of the compound was beginning to diminish by 48 h. Continuous exposure to small amounts of compound may be more effective than an acute exposure to a higher concentration of agent. To determine the effect of treatment on cell motility, comparisons were made between groups and time-points (intertreatment analysis). Interestingly, higher amounts of C3R increased cell motility (100 μM C3R; $p = 0.0138$) when compared to the group treated with 25 μM at 48 h, suggesting either a C3R desensitization or a biphasic effect on cell motility. Hence, we concluded that low amounts of C3R, perhaps even lower than 25 μM, may be needed to impart more than just a modest delay in cell motility (Fig. 3SA).

Importantly, no significant change in AlamarBlue® staining was observed when similar treatments were employed, suggesting that C3R exerted no influence on the viability of RKO cells (Fig. 3SB). This finding indicated that the C3R present in lyophilized AP compound (at the tested concentrations) was not cytotoxic to RKO cells.

3.3. AP feeding during and after induction of acute inflammation

Despite extensive loss of body weight and severe diarrhea, no animals died within the first few days following the induction of acute inflammation by intrarectal delivery (single administration) of TNBS (Table 1S). Acute inflammation generated a lesion with macroscopic evidence of necrosis and microscopically characterized by a coagulative necrosis process at the site of TNBS instillation. No statistical difference was observed among the groups with respect to macro and microscopic evaluation of acute inflammation 48 h after TNBS instillation (Table 2S).

The change in body weight over time did not differ significantly among the treatment groups after the induction of colitis (Table 1S). Intake of both food and water after 25 weeks was lower in the groups treated with lyophilized AP (G3 and G4) as compared to the untreated group (G1) ($p < 0.001$) (Table 3S). Among the groups fed lyophilized AP, food intake was lower in the group (G4) receiving the highest dose of AP (7.5%), ($p < 0.001$) (Table 3S). The average consumption of lyophilized AP was 0.994 ± 0.18 and 1.44 ± 0.25 g/rat/day in the in groups fed 5.0% and 7.5%, respectively (Table 3S). ALT serum levels and relative liver weight (g) indicated that AP feeding did not present liver toxicity to the animals in this experiment (Fig. 4S).

3.4. AP intake effectively reduced ACF development

Both dietary AP interventions, as well as NAC (0.2%), reduced the total number of AC as compared to the untreated group (G1) ($p < 0.001$). AP feeding at 5.0% (G3) reduced the total number of ACF ($p < 0.001$) as compared to the untreated group (G1). With respect to ACF multiplicity, treatment with AP 5.0% (G3) and 0.2% NAC (G4) reduced the number of ACF with 4-10 AC (Fig. 3A) as compared to the untreated group (G1) ($p < 0.001$). In addition, ingestion of both AP and NAC 0.2% (G2-G4) decreased the number of large ACF (> 10 AC) as compared to the untreated group G1 ($p < 0.001$) (Table 2). These results suggest that AP treatment can potentially reduce tumor burden.

3.5. AP influenced tumor incidence and cell proliferation

Histopathological analyses of colon tumors revealed no difference in mean tumor multiplicity (Table 2). Nonetheless, treatment with 5.0% AP (G3) led to a reduction in the incidence of colonic tumors with high-grade dysplasia (Fig. 3D) (13,16%) and, consequently, an increase in colon tumors with low grade dysplasia (86,84%) as compared to control group (G1) (Fig. 3C) (Table 2).

Colon tumors in all groups showed typical nuclear immunolocalization of Ki-67 (Figs. 3B and 2S). Cell proliferation (Ki-67 LI %) was reduced in colon tumors from animals administered 7.5% AP (G4: 59.88 ± 14.84) and 0.2% NAC (57.34 ± 15.39) (G2), as compared to controls (G1) (71.23 ± 10.56) ($p < 0.001$) (Table 2, Figs. 1S and 2S). No difference in apoptotic index, connexin 43 or β-catenin immuno expression was observed between groups (data not shown). This result suggests that AP feeding reduced cell proliferation in colon tumors obtained in the *in vivo* bioassay.

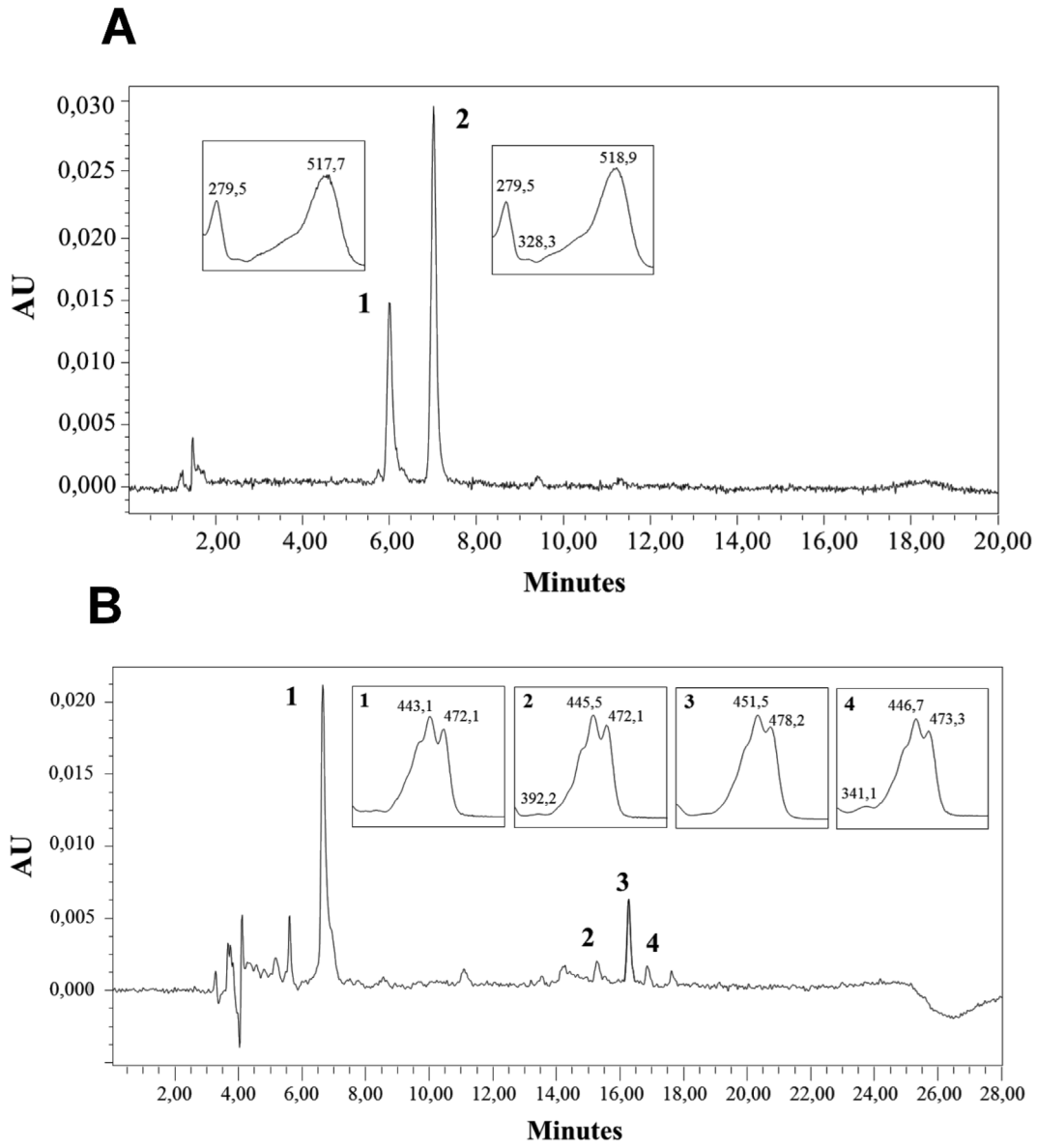

Fig. 2. Chromatograms and UV–Vis spectra of **(A)** anthocyanins [peak identification: (1) cyanidin 3-glucoside and (2) cyanidin 3-rutinoside] and **(B)** carotenoids [peak identification: (1) lutein, (2) α-carotene, (3) β-carotene e (4) 9-cis β-carotene] obtained via HPLC.

Table 1
Phytochemical composition of lyophilized AP.

Phytochemical composition	Concentration*
Anthocyanins	**mg/100 g AP**
Cyanidin 3-glucoside (C3G)	110.10 ± 4.39
Cyanidin 3-rutinoside (C3R)	214.09 ± 17.32
Total	324.19 ± 21.71
Carotenoids	**μg/100 g AP**
Lutein	367 ± 142.12
α-carotene	458 ± 2.82
β-carotene	1908.5 ± 4.24
13-cis β-carotene	55.5 ± 37.47
9-cis β-carotene	365 ± 2.12
Total	4234.5 ± 7.07

AP = açaí fruit pulp. *For the phytochemical composition, AP analysis was performed in triplicate. Data are expressed as the Mean ± Standard Deviation (SD). Underlined components corresponded to the most common for each category: Anthocyanins, Carrotenoids or others.

3.6. Tumor gene expression was altered by AP feeding

Gene expression analyses were conducted in an attempt to better understand the potential mechanisms by which AP inhibited tumor growth. Out of the 91 genes included in the TaqMan® Array Cards (TAC) (Table 4S), six genes were significantly differentially expressed when the control group, G1, was compared to the groups fed AP (G3 and G4) (Fig. 4). MutS homolog 6 (*Msh6*) was downregulated in colon tumors from rats fed only basal diet vs. 5.0% AP (G1 vs G3; $p = 0.04$). All of the other altered genes were upregulated in colon tumors from rats fed 7.5% AP (G1 vs G4). These genes included: Peroxisome proliferator activated receptor alpha (*Ppara*), Akt serine/threonine kinase 3 (*Akt3*), Dlc1 Rho GTPase activating protein (*Dlc1*) and vascular endothelial growth factor D (*Vegfd*). Genes upregulated in colon tumors from rats fed 0.2% NAC (e.g., G1 vs G2) were free fatty acid receptor 2 (*Ffar2*) and *Ppara* (Fig. 4). These results suggest that both common (*Ppara*) and independent mechanisms may play a central role in the activity of NAC vs. AP.

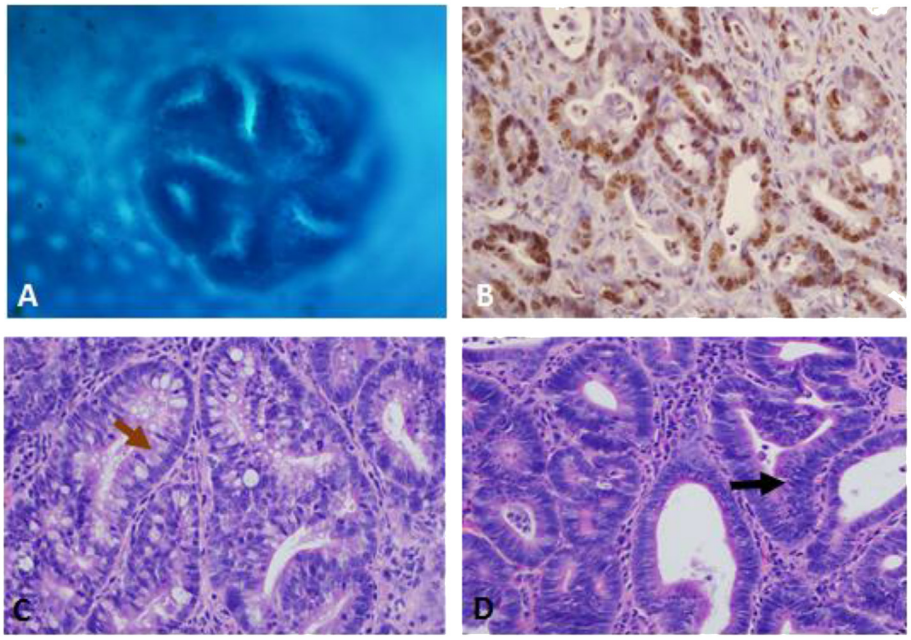

Fig. 3. (A) Representative topographic view of classic ACF in a methylene blue-stained colon whole-mount containing nine aberrant crypts (40×); **(B)** Representative Ki-67 immunostaining (brown nuclei) in a colon tumor (20×); **(C)** Representative microscopic view of low grade dysplasia tumor. Brown arrow indicates the crypt epithelium containing uniform, crowded and basally located nuclei and sparse goblet cells (40×); **(D)** Representative microscopic view of one tumor with high grade dysplasia. Black arrow shows the nuclear pseudostratification. (40×). (For interpretation of the references to color in this figure legend, the reader is referred to the Web version of this article.)

4. Discussion

Findings of the present study indicate that lyophilized açaí fruit and its main phytochemical compound can reduce colon carcinogenesis associated with acute inflammation in rats, as well as modify the motility of human RKO colorectal carcinoma cells *in vitro*. Firstly, the findings show that the lowest concentration of C3R (25 μM), the main anthocyanin identified in lyophilized AP, has the potential to reduce cell motility, as analyzed by the wound healing assay, at low concentrations. Secondly, lyophilized AP intake reduced total pre-neoplastic ACF, ACF multiplicity (ACF 1-4 crypts and ACF > 10 crypts), tumor cell proliferation, and the incidence of tumors with high-grade dysplasia. Thirdly, lyophilized AP modulated the expression of six genes involved in various hallmarks of cancer.

The phytochemical analyses demonstrate that the lyophilized AP used in the *in vivo* experiment had high levels of cyanidin 3-rutinoside (C3R) and cyanidin 3-glusoside (C3G). This finding is in agreement with several others that report the same anthocyanins in açaí pulp (Schauss et al., 2006; Romualdo et al., 2015). In addition, the amount of anthocyanins may vary among açaí samples used in different studies (Ribeiro et al., 2010; Romualdo et al., 2015). Moreover, the level of carotenoids (4.23 mg/100 g) in the lyophilized AP used in the present study was higher than that reported by others for different açaí samples (Ribeiro et al., 2010; Romualdo et al., 2015).

In our previous study, we investigated the potential protective effect of a commercial product formulated as a spray-dried açaí pulp against a sporadic colon cancer rat model (Fragoso et al., 2013). This spray-dried açaí powder is rich in anthocyanins but possesses varying amounts of maldextrin, a carrier agent used in industrial processing (Tonon et al., 2010; Fragoso et al., 2013; Romualdo et al., 2015). The lyophilized AP used in this study is a rich source of anthocyanins as well, however it is free of any type of food additives (Table 1).

The metastatic cascade is a multi-step process, characterized by tumor cell invasion, followed by colonization at distal sites (Van Zijl et al., 2011). Increased cell motility is one of the requirements that cancer cells must acquire in order to proceed with the metastatic cascade (Chen et al., 2006; Van Zijl et al., 2011). Since our *in vivo* 25-week model does not mimic the metastatic step, we decided to analyze it using an *in vitro* approach. Following characterization of the anthocyanin composition of lyophilized AP, cyanidin 3-rutinoside (C3R) was

Table 2
Effects of lyophilized AP intake on ACF and tumor development.

Groups	(G1) Untreated	(G2) 0.2% NAC	(G3) 5.0% AP	(G4) 7.5% AP
ACF data				
Number of rats	14/15	10/10	15/15	15/15
Total ACF/colon	222.4 ± 48.5	166.4 ± 47.8	138.0 ± 49.7*	173.7 ± 59.2
Total AC	1366.8 ± 31.5	914.4 ± 290.7*	790.5 ± 337.7*	1004.3 ± 354.3*
ACF Multiplicity				
ACF 1-3	80.1 ± 31.5	74.9 ± 23.36	53.5 ± 18.0	66.0 ± 30.78
ACF 4-10	100.57 ± 23.53	62.9 ± 16.9*	62.07 ± 26.45*	79.4 ± 28.0
ACF > 10	41.71 ± 13.24	25.70 ± 11.38*	21.47 ± 12.26*	27.60 ± 11.21*
Tumor data				
Tumor-bearing rats	10/15	5/10	12/15	12/15
KI-67 LI%	71.23 ± 10.56	57.34 ± 15.39*	67.24 ± 13.99	59.87 ± 14.80*
Mean number of tumors	2.33 ± 2.19	1.50 ± 1.90	2.53 ± 2.45	1.67 ± 1.50
Tumor multiplicity	3.50 ± 1.72	3.0 ± 1.58	2.58 ± 2.15	2.08 ± 1.38
Tumor incidence (%)				
Low Grade Dysplasia	60	80	87*	76
High Grade Dysplasia	40	20	13*	24

Total ACF, Total AC and ACF multiplicity were counted and are refereed as units (U). ACF data and Tumor data are expressed as Mean ± Standard Deviation (SD) and analyzed by ANOVA followed by Tukey *post hoc* test. Tumor incidence was analyzed by Chi-square's exact test. AP = açaí pulp. *Different from G1 ($p < 0.05$).

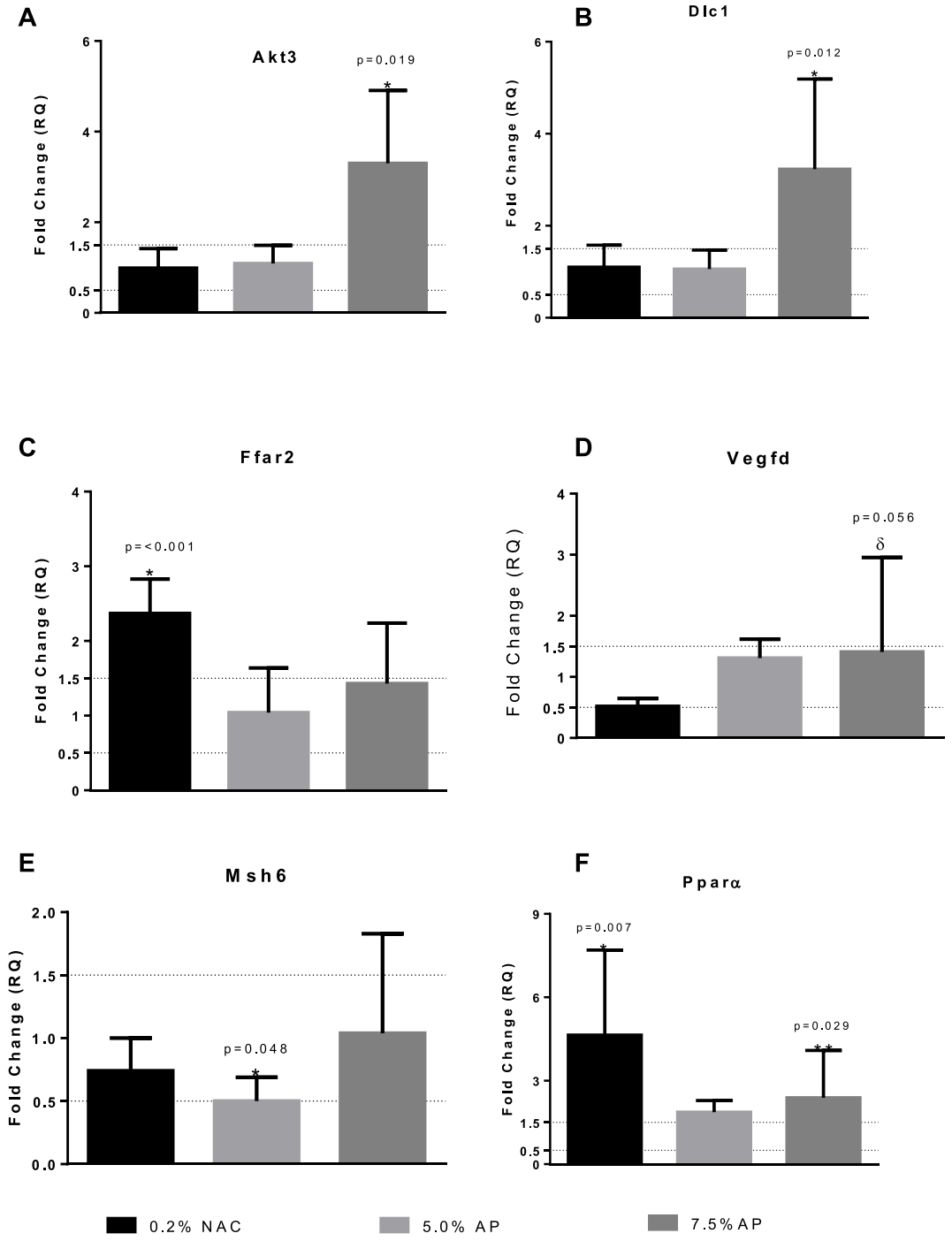

Fig. 4. Relative quantitation of genes differently expressed in tumors treated with 5.0 and 7.5% AP and 0.2% NAC. Five samples per group were used for the gene expression analysis. All conditions were contrasted against the untreated group (*t*-test). Data are expressed as Mean ± Standard Deviation (SD).

selected for testing in the wound healing assay *in vitro*. A slight reduction in cell motility was observed in cells treated with 25 μM C3R between 24 h and 48 h ($p = 0.579$). The lowest concentration of C3R caused a more efficient reduction in the motility of RKO cells, suggesting that this cyanidin can decrease cell motility, directly involved in the metastatic process. Also, our results are in according with Chen et al. (2006) that showed that C3R decreases invasiveness of highly metastatic A549 human lung carcinoma cells *in vitro* in absence of cytotoxicity. Thus, it is possible that lower concentrations of C3R and chronic treatments may be needed to achieve an optimal biological response. A crude extract of anthocyanins has shown efficiency in reducing the motility of CAL 27 oral cancer cells (Fan et al., 2015). In their study, the authors tested different concentrations of crude anthocyanin extract from black rice (*Oryza sativa* L.) where the lowest concentration (100 μg/mL) reduced cell motility after 6 h of treatment. In our experiment, pure C3R, when used at a lower concentration (~15.7 μg/mL), also demonstrated a tendency to reduce cell motility. Thus, this suggests that C3R is a compound with a strong capacity to reduce cell motility at low concentrations; higher amounts may cause a desensitization effect. Use of C3R in combination with other polyphenols and/or carotenoids, may increase its antitumor activity. This point is important because the presence of anthocyanin and carotenoids in the lyophilized AP may explain the discrepancies observed between *in vivo* and *in vitro* results and could also be responsible for açaí's

antioxidant capacity and anti-tumor activity (Schauss et al., 2006; Fragoso et al., 2013).

Aberrant Crypt Foci (ACF) are preneoplastic lesions that can be easily identified in methylene blue-stained colon wholemounts (Bird and Good, 2000). ACF with a high number of AC and high multiplicity are more likely to progress to advanced lesions during colorectal carcinogenesis (Bird and Good, 2000). Stereological analyses of ACF showed that the lyophilized AP reduced the total number of AC and multiplicity of ACF, as well as tumor incidence, by reducing those tumors with high-grade dysplasia. These results suggest that intake of lyophilized AP attenuates the promotion/progression of colon carcinogenesis associated with acute colitis, as demonstrated previously (Choi et al., 2016).

Among the genes with differential expression identified in this study, three presented a direct correlation with the other results of this study. We can infer that AP increased the gene expression of negative regulators of cell proliferation such as *Dlc1* and *Akt3*, as well as inflammatory genes (*Ppara*). To support this information, it is necessary to understand the role of these genes in cell biology.

Dlc1 is a gene that encodes a Rho GTPase-activating protein (RhoGAP), responsible for catalyzing the hydrolysis of GTP into GDP, rendering the RhoGTPases inactive (Lahoz and Hall, 2008). This gene has been identified as a tumor suppressor in several types of cancer (Vigil et al., 2010) and two independent studies have provided evidence for its role in cancer (Wu et al., 2009; Denholm et al., 2005). Our results show that administration of AP (7.5%) increased *Dlc1* expression in tumors (Fig. 4). Upregulation of this gene could contribute to the ability of high-dose AP to reduce cell proliferation, as indicated by the lowest Ki-67 LI and associated cellular protection.

Peroxisome proliferator-activated receptors (PPARs) are a family of nuclear receptors that comprise three isoforms: PPARα, PPARβ and PPARγ (Panigrahy et al., 2008). *PPARα* is involved in lipid metabolism, inflammation, cell cycle progression and angiogenesis (Panigrahy et al., 2008). Investigation of its inflammatory role in C57BL/6 mice revealed that PPARα, their ligands and the respective activated genes downregulate activated nuclear transcription factor-κB (*NF-κB*) and its target genes (*Il6*, *Il12* and *Cox2*) (Poynter and Daynes, 1998). Administration of agents capable of activating *Ppara* to aged mice restored the cellular redox balance by lowering tissue lipid peroxidation, eliminating activate NF-κB and inducing loss of spontaneous inflammatory cytokine production (Poynter and Daynes, 1998). The *Ppara* gene was the only gene identified in the present study that was upregulated in both animals treated with NAC or 7.5% AP (Fig. 4). Hence, it is possible that the observed effects of AP in controlling tumor burden could be explained by the ability of *PPARα* to reduce NF-κB expression.

AKT plays an important role in apoptosis inhibition, cell proliferation, metastasis, drug resistance, metabolism and radiation resistance (Haggblad-Sahlberg et al., 2016). This protein is commonly activated in human cancers, stimulating cell proliferation and survival. For this reason, inhibitors of this protein may have therapeutic value (Haggblad-Sahlberg et al., 2016). This gene is involved in the PI3K pathway, one of the pathways affected in the AOM/DSS model of colitis-associated colorectal cancer (Josse et al., 2014).

The three isoforms of AKT protein (AKT1, AKT2 and AKT3) share a high degree of homology, are expressed from different genes and have different physiological functions and expression patterns (Haggblad-Sahlberg et al., 2016). Hollander et al., (2011) analyzed the role of each of the three isoforms of AKT in *K-ras* mediated lung tumorigenesis, using genetically engineered deficient mice. They concluded that *AKT1* prevented the development of tumors, while deletion of *AKT3* increased tumor initiation and progression.

Similar to the *Dlc1* gene, *AKT3* appears to play a protective role in the colon carcinogenesis model used in this study, as in the AOM/DSS model (Clapper et al., 2007). Since this protein is involved in pathways that are important in colon carcinogenesis, AKT3 most likely acts as a tumor suppressor by indirectly regulating the Wnt pathway and, consequently, reducing tumor cell proliferation. Taken together, expression analyses of these specific genes may explain the observed reduction in tumor cell proliferation as indicated by a decrease in Ki-67 LI.

In summary, our findings suggest that lyophilized açaí pulp confers cellular protection in the rat model of colitis-associated colon carcinogenesis. In addition, these results confirm, for the first time, the beneficial effect of lyophilized açaí pulp in the colitis model based on macroscopic, microscopic and molecular colon tumor analyses.

Conflict of interest

The authors declare that they have no conflict of interest.

Acknowledgments

Mariana F. Fragoso was the recipient of a fellowship from FAPESP (2013/17600-0) and CAPES (PDSE 008192/2014-06). Luis F. Barbisan was the recipient of a research grant from PROAP/CAPES. The authors thank Renata Galhardo Borguini and Manuela Cristina Pessanha de Araújo Santiago (Embrapa Food Technology, Guaratiba, Rio de Janeiro, RJ, Brazil) for açaí phytochemical analysis.

Appendix A. Supplementary data

Supplementary data related to this article can be found at https://doi.org/10.1016/j.fct.2018.08.078.

Transparency document

Transparency document related to this article can be found online at https://doi.org/10.1016/j.fct.2018.08.078.

References

Amrouche-Mekkioui, I., Djerdjouri, B., 2012. N-acetylcysteine improves redox status, mitochondrial dysfunction, mucin-depleted crypts and epithelial hyperplasia in dextran sulfate sodium-induced oxidative colitis in mice. Eur. J. Pharmacol. 691 (1–3), 209–217. http://doi.org/10.1016/j.ejphar.2012.06.014.

Bird, R.P., Good, C.K., 2000. The significance of aberrant crypt foci in understanding the pathogenesis of colon cancer. Toxicol. Lett. 112–113, 395–402.

Clapper, M.L., Cooper, H.S., Chang, W.-C.L., 2007. Dextran sulfate sodium-induced colitis-associated neoplasia: a promising model for the development of chemopreventive interventions. Acta Pharmacol. Sin. 28, 1450–1459. https://doi.org/10.1111/j.1745-7254.2007.00695.x.

Chen, P.N., Chu, S.C., Chiou, H.L., Kuo, W.H., Chiang, C.L., Hsieh, Y.S., 2006. Mulberry anthocyanins, cyanidin 3-rutinoside and cyanidin 3-glucoside, exhibited an inhibitory effect on the migration and invasion of a human lung cancer cell line. Canc. Lett. 235 (2), 248–259. https://doi.org/10.1016/j.canlet.2005.04.033.

Choi, Y.J., Choi, Y.J., Kim, N., Nam, R.H., Lee, S., Lee, H.S., et al., 2016. Açaí berries inhibit colon tumorigenesis in azoxymethane/dextran sulfate sodium-treated mice. Gut and Liver 1–11.

Das, D., Arber, N., Jankowski, J.A., 2007. Chemoprevention of colorectal cancer. Digestion 76 (1), 51–67. http://doi.org/10.1159/000108394.

Denholm, B., Brown, S., Ray, R.P., Ruiz-Gómez, M., Skaer, H., Castelli-Gair Hombría, J., 2005. Crossveinless-c is a RhoGAP required for actin reorganisation during morphogenesis. Development 132 (10), 2389–2400.

Fan, M.-J., Wang, I.-C., Hsiao, Y.-T., Lin, H.-Y., Tang, N.-Y., Hung, T.-C., et al., 2015. Anthocyanins from black rice (Oryza sativa L.) demonstrate antimetastatic properties by reducing MMPs and NF-κB expressions in human oral cancer CAL 27 cells. Nutr. Canc. 67 (2), 327–338.

Femia, A. Pietro, Caderni, G., 2008. Rodent models of colon carcinogenesis for the study of chemopreventive activity of natural products. Planta Med. 74 (13), 1602–1607. http://doi.org/10.1055/s-2008-1074577.

Feng, B., Dong, T.T., Wang, L.L., Zhou, H.M., Zhao, H.C., Dong, F., Zheng, M.H., 2012. Colorectal cancer migration and invasion initiated by microRNA-106a. PLoS One 7 (8), 1–9. http://doi.org/10.1371/journal.pone.0043452.

Fragoso, M.F., Romualdo, G.R., Ribeiro, D. a, Barbisan, L.F., 2013. Açai (Euterpe oleracea Mart.) feeding attenuates dimethylhydrazine-induced rat colon carcinogenesis. Food Chem. Toxicol. 58, 68–76. http://doi.org/10.1016/j.fct.2013.04.011.

Haggblad Sahlberg, S., Mortensen, A., Haglof, J., Engskog, M., Arvidsson, T., Pettersson, C., et al., 2016. Different functions of AKT1 and AKT2 in molecular pathways, cell migration and metabolism in colon cancer cells. Int. J. Oncol. 1–10.

Hamilton, S.R., Aaltonen, L.A., 2000. World Health Organization Classification of Tumors Pathology and Genetics, vol. 6. IARC Press, pp. 103 220.

Hendry, G.A.F., Houghton, J.D., 1992. Natural Food Colorants. Blackie Academic, London, pp. 183–241.
Hollander, M.C., Maier, C.R., Hobbs, E.A., Ashmore, A.R., Linnoila, R.I., Dennis, P.A., 2011. Akt1 deletion prevents lung tumorigenesis by mutant mutant K-ras. Oncogene 30, 1812–1821.
INCA, 2016. Instituto Nacional do Câncer - estatística sobre a incidência de câncer colorretal na população brasileira. Brasil. http://www.inca.gov.br/estimativa/2016/, Accessed date: 2 October 2016.
Josse, C., Bouznad, N., Geurts, P., Irrthum, A., Huynh-Thu, V.A., Servais, L., Oury, C., 2014. Identification of a microRNA landscape targeting the PI3K/Akt signaling pathway in inflammation-induced colorectal carcinogenesis. Am. J. Physiol. Gastrointest. Liver Physiol. 306 (3), G229–G243.
Kahyat, T., 2005. Comportamento de risco para doença aterosclerótica coronariana na população de Inhangapí cuja base alimentar é o fruto do açaí (Euterpe oleracea). Universidade Federal do Pará. Curso de Medicina, Departamento de Clínica Médica, Belém do Pará (in Portuguese).
Lahoz, A., Hall, A., 2008. DLC1: a significant GAP in the cancer genome. Genes Dev. 22 (13), 1724–1730.
Livak, K.J., Schmittgen, T.D., 2001. Analysis of relative gene expression data using real-time quantitative PCR and. Methods 25, 402–408. http://doi.org/10.1006/meth.2001.1262.
Lofano, K., Principi, M., Scavo, M.P., Pricci, M., Ierardi, E., Di Leo, A., 2012. Dietary lifestyle and colorectal cancer onset, recurrence, and survival: myth or reality? J. Gastrointest. Canc. 44, 1–11. http://doi.org/10.1007/s12029-012-9425-y.
Milani, A., Basirnejad, M., Shahbazi, S., Bolhassani, A., 2017. Carotenoids: biochemistry, pharmacology and treatment. Br. J. Pharmacol. 174 (11), 1290–1324. http://doi.org/10.1111/bph.13625.
Panigrahy, D., Kaipainen, A., Huang, S., Butterfield, C.E., Barnés, C.M., Fannon, M., et al., 2008. PPARalpha agonist fenofibrate suppresses tumor growth through direct and indirect angiogenesis inhibition. Proceedings of the National Academy of Sciences of theU S A 105 (3), 985–990.
Paz, M., Gúllon, P., Barroso, M.F., Carvalho, A.P., Domingues, V.F., Gomes, et al., 2015. Brazilian fruit pulps as functional foods and additives: evaluation of bioactive compounds. Food Chem. 172, 462–468. http://doi.org/10.1016/j.foodchem.2014.09.102.
Poynter, M.E., Daynes, R.A., 1998. Peroxisome proliferator-activated receptor alpha activation modulates cellular redox status, represses nuclear factor-kappa B signaling, and reduces inflammatory cytokine production in aging. J. Biol. Chem. 273 (49), 32833–32841.
Ribeiro, J.C., Antunes, L.M.G., Aissa, A.F., Darin, J.D.C., De Rosso, V.V., Mercadante, A.Z., et al., 2010. Evaluation of the genotoxic and antigenotoxic effects after acute and subacute treatments with açai pulp (Euterpe oleracea Mart.) on mice using the erythrocytes micronucleus test and the comet assay. Mutat. Res. 695 (1–2), 22–28.
Rodriguez-Amaya, D.B., 2001. A Guide to Carotenoid Analysis in Foods, first ed. ILSI Press, Washington.
Romualdo, G.R., Fragoso, M.F., Borguini, R.G., de Araújo Santiago, M.C.P., Fernandes, A.A.H., Barbisan, L.F., 2015. Protective effects of spray-dried açaí (Euterpe oleracea Mart) fruit pulp against initiation step of colon carcinogenesis. Food Res. Int. 77, 432–440. http://doi.org/10.1016/j.foodres.2015.08.037.
Santiago, C., Pagán, B., Isidro, A. a, Appleyard, C.B., 2007. Prolonged chronic inflammation progresses to dysplasia in a novel rat model of colitis-associated colon cancer. Canc. Res. 67 (22), 10766–10773. http://doi.org/10.1158/0008-5472.CAN-07-1418.
Schauss, A.G., Wu, X., Prior, R.L., Ou, B., Huang, D., Owens, J., et al., 2006. Antioxidant capacity and other bioactivities of the freeze-dried Amazonian palm berry, Euterpe oleraceae mart. (acai). J. Agric. Food Chem. 54 (22), 8604–8610. http://doi.org/10.1021/jf0609779.
Tonon, R.V., Brabet, C., Hubinger, M.D., 2010. Anthocyanin stability and antioxidant activity of spray-dried açai (Euterpe oleracea Mart.) juice produced with different Carrier agents. Food Res. Int. 43 (3), 907–914.
Torre, L.A., Bray, F., Siegel, R.L., Ferlay, J., Lortet-tieulent, J., Jemal, A., 2015. Global cancer statistics, 2012. CA: A Canc. J. Clin. 65 (2), 87–108. http://doi.org/10.3322/caac.21262.
Torres, T., Farah, A., 2016. Coffee, matte, açaí and beans are the main contributors to the antioxidant capacity of Brazilian's diet. Eur. J. Nutr. 1–11. http://doi.org/10.1007/s00394-016-1198-9.
Vandesompele, J., De Preter, K., Poppe, B., Van Roy, N., De PaCe, A., 2002. Accurate Normalization of Real-time Quantitative RT -PCR Data by Geometric Averaging of Multiple Internal Control Genes, vols. 1–12.
Van Zijl, F., Krupitza, G., Mikulits, W., 2011. Initial steps of metastasis: cell invasion and endothelial transmigration. Mutat. Res. 728, 23–34. https://doi.org/10.1016/j.mrrev.2011.05.002.
Vigil, D., Cherfils, J., Rossman, K.L., Der, C.J., 2010. Ras superfamily GEFs and GAPs: validated and tractable targets for cancer therapy? Nat. Rev. Canc. 10 (12), 842–857.
Wu, P., Jin, Y., Shang, Y., Jin, Z., Wu, P., Huang, P., 2009. Restoration of DLC1 gene inhibits proliferation and migration of human colon cancer HT29 cells. Annual and Clinical Laboratory Science 39 (3), 263–269.
Yamaguchi, K.K.L., Pereira, L.F.R.,R., Lamarão, C.V., Lima, E.S., Veiga-Junior, V.F., 2015. Amazon acai: chemistry and biological activities: a review. Food Chem. 179, 137–151. http://doi.org/10.1016/j.foodchem.2015.01.055.